Resource

Cell Reports

Multi-level Strategy for Identifying Proteasome-Catalyzed Spliced Epitopes Targeted by CD8$^+$ T Cells during Bacterial Infection

Graphical Abstract

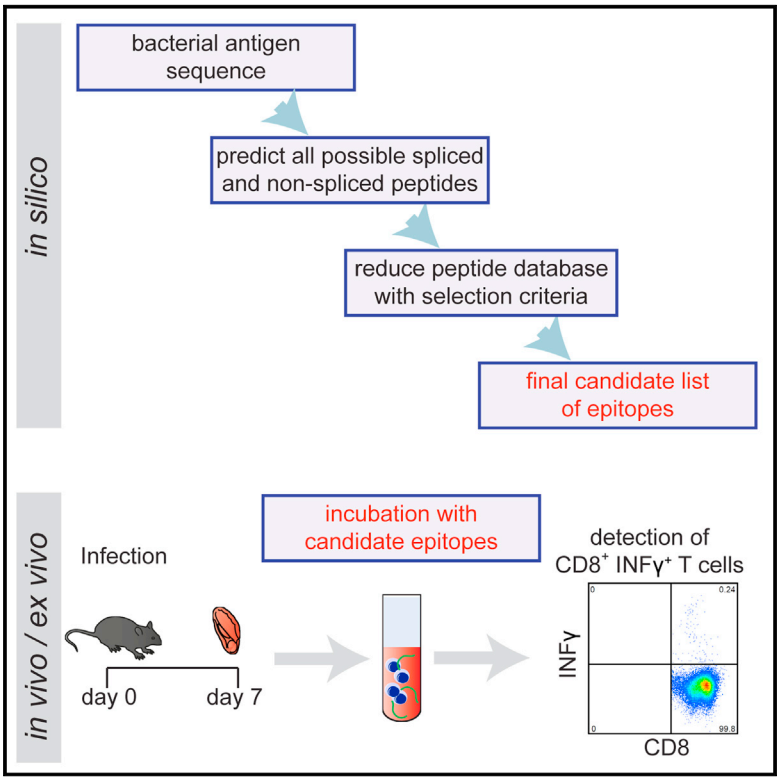

Highlights

- Development of in-silico-based, multi-level strategy for identifying spliced epitopes
- Developed strategy identifies two spliced bacterium-derived CD8$^+$ T cell epitopes
- Proteasome-catalyzed peptide splicing increases the pathogen-derived peptide pool

Authors

Anouk C.M. Platteel, Juliane Liepe, Kathrin Textoris-Taube, ..., Peter M. Kloetzel, Michele Mishto, Alice J.A.M. Sijts

Correspondence

michele.mishto@kcl.ac.uk (M.M.), e.j.a.m.sijts@uu.nl (A.J.A.M.S.)

In Brief

Proteasomes both degrade proteins and ligate generated products, creating "spliced peptides" composed of distant protein parts. Platteel et al. now describe a multi-level strategy for identifying proteasome-generated spliced T cell epitopes. This work suggests ways of defining spliced epitopes within any antigen of interest and to determine their immunological relevance.

Platteel et al., 2017, Cell Reports *20*, 1242–1253
August 1, 2017
http://dx.doi.org/10.1016/j.celrep.2017.07.026

CellPress

OPEN ACCESS
CellPress

Cell Reports
Resource

Multi-level Strategy for Identifying Proteasome-Catalyzed Spliced Epitopes Targeted by CD8+ T Cells during Bacterial Infection

Anouk C.M. Platteel,[1,8] Juliane Liepe,[2,3,8] Kathrin Textoris-Taube,[4,5,6] Christin Keller,[4,5] Petra Henklein,[4] Hanna H. Schalkwijk,[1] Rebeca Cardoso,[1] Peter M. Kloetzel,[4,5] Michele Mishto,[4,5,7,9,*] and Alice J.A.M. Sijts[1,9,10,*]

[1]Division of Immunology, Faculty of Veterinary Medicine, Utrecht University, 3571 EK Utrecht, the Netherlands
[2]Centre for Integrative Systems Biology and Bioinformatics, Department of Life Sciences, Imperial College London, SW7 2AZ London, UK
[3]Max-Planck-Institute for Biophysical Chemistry, 37077 Göttingen, Germany
[4]Institut für Biochemie, Charité - Universitätsmedizin Berlin, 10117 Berlin, Germany
[5]Berlin Institute of Health, 10117 Berlin, Germany
[6]Shared Facility for Mass Spectrometry, Charité - Universitätsmedizin Berlin, 10117 Berlin, Germany
[7]Centre for Inflammation Biology and Cancer Immunology (CIBCI) & Peter Gorer Department of Immunobiology, King's College London, SE1 1UL London, UK
[8]These authors contributed equally
[9]Senior author
[10]Lead Contact
*Correspondence: michele.mishto@kcl.ac.uk (M.M.), e.j.a.m.sijts@uu.nl (A.J.A.M.S.)
http://dx.doi.org/10.1016/j.celrep.2017.07.026

SUMMARY

Proteasome-catalyzed peptide splicing (PCPS) generates peptides that are presented by MHC class I molecules, but because their identification is challenging, the immunological relevance of spliced peptides remains unclear. Here, we developed a reverse immunology-based multi-level approach to identify proteasome-generated spliced epitopes. Applying this strategy to a murine *Listeria monocytogenes* infection model, we identified two spliced epitopes within the secreted bacterial phospholipase PlcB that primed antigen-specific CD8+ T cells in *L. monocytogenes*-infected mice. While reacting to the spliced epitopes, these CD8+ T cells failed to recognize the non-spliced peptide parts in the context of their natural flanking sequences. Thus, we here show that PCPS expands the CD8+ T cell response against *L. monocytogenes* by exposing spliced epitopes on the cell surface. Moreover, our multi-level strategy opens up opportunities to systematically investigate proteins for spliced epitope candidates and thus strategies for immunotherapies or vaccine design.

INTRODUCTION

CD8+ T cell responses play an important role in the clearance of intracellular pathogens and in protection from subsequent infections. CD8+ T cells react to epitopes presented by major histocompatibility complex class I (MHC class I) molecules at the cell surface. Epitope generation usually starts through proteasomal processing of pathogen-derived intracellular proteins. Peptides released by the proteasome are translocated by the transporter associated with antigen processing (TAP) into the endoplasmic reticulum (ER), where they may undergo N-terminal trimming by ER-resident aminopeptidases (ERAPs) (Cascio et al., 2001; Rock et al., 1994; Sijts and Kloetzel, 2011) and are loaded onto MHC class I molecules for presentation at the cell surface (Groettrup et al., 2010).

Given the central role of proteasomes in MHC class I antigen processing, their catalytic activity plays a fundamental role in shaping the pathogen-derived peptide repertoire toward which CD8+ T cells may react. The catalytic activity of proteasomes is displayed by three subunits, β1, β2, and β5, which are replaced by the induced catalytic subunits β1i/LMP2, β2i/MECL1, and β5i/LMP7 when cells are exposed to an inflammatory milieu (Groettrup et al., 2010; Sijts and Kloetzel, 2011). The changes in the catalytic subunit composition induce subtle modifications in conformation of the active sites, which affect proteasome proteolytic dynamics, and have consequences for the quantities of peptides produced (Arciniega et al., 2014; Liepe et al., 2015; Mishto et al., 2014; Ruschak and Kay, 2012; Sijts et al., 2000). Proteasomes can simply hydrolyze the peptide bonds of the antigen, thereby releasing canonical non-spliced peptides, or splice two distal fragments of the antigen, thereby generating peptides with a novel sequence (Vigneron et al., 2004). The latter mechanism is called proteasome-catalyzed peptide splicing (PCPS) (Mishto et al., 2012).

Despite the well-established crucial role of proteasomes in MHC class I antigen processing, the immunological relevance of PCPS is still a matter of debate, in part because only a few proteasome-generated spliced epitopes, mainly derived from tumor-associated antigens (Dalet et al., 2011; Ebstein et al., 2016; Hanada et al., 2004; Michaux et al., 2014; Vigneron et al., 2004; Warren et al., 2006), have been described so far. Some recent studies, however, hint at the importance of PCPS in MHC class I antigen presentation. Indeed, based on mass spectrometry (MS) analyses, approximately one-third of the peptides presented by MHC class I molecules on human lymphoblastoid

and fibroblast cells are proteasome-generated spliced peptides, and one-third of self-antigens presented by MHC class I on these cells are represented by spliced peptides only (Liepe et al., 2016). Such a significant increase in the variety of peptides potentially recognized by $CD8^+$ T cells due to PCPS is also strengthened by their amount, which has been calculated in the order of one fourth of the MHC class I-restricted self-peptides (Liepe et al., 2016). This is in agreement with the amount of tumor-associated spliced epitopes presented by human MHC class I molecules at the cell surface, as shown for the $gp100^{mel}$ antigen (Ebstein et al., 2016).

The relevance of PCPS in the cell-mediated immune response during infections is still unknown. We recently described cross-reactivity of $CD8^+$ T cells, primed during *L. monocytogenes* by the dominant listeriolysin O (LLO)-derived epitope $LLO_{296–304}$, toward the spliced epitope $LLO_{294/297–304}$ (Platteel et al., 2016). Nevertheless, so far, no clear evidence that PCPS leads to spliced peptide-specific $CD8^+$ T cell responses during infection has been found. The scarcity of knowledge on the role of PCPS in immune recognition illustrates the difficulty of identifying immunologically relevant spliced epitopes, which lies in adopting a reverse immunology approach, requiring a complex in silico-in vitro workflow. To propel further investigation into the role of PCPS in antigen processing, we have developed a multi-level spliced epitope identification strategy, which we tested in the murine *L. monocytogenes* infection model. *L. monocytogenes* is a Gram-positive bacterium that primarily infects phagocytes and then mobilizes the host cell cytoskeleton to spread to neighboring cells. To enter the cytosol of infected cells, the bacteria secrete LLO and the phospholipases PlcA/phosphatidylinositol-specific phospholipase C (PI-PLC) and PlcB/phosphatidylcholine-preferring phospholipase C (PC-PLC) (Bielecki et al., 1990; Pamer, 2004; Portnoy et al., 1992). Bacterial clearance during *L. monocytogenes* infection is mediated by $CD8^+$ T cells specific for the secreted bacterial proteins. Therefore, to test and validate our spliced epitope identification approach, we decided to use the secreted PlcA and PlcB proteins as model antigens.

RESULTS

Identification of *L. monocytogenes*-Derived Spliced Epitope Candidates

$LLO_{296–304}$ and its spliced variant $LLO_{294/297–304}$ are the main, known, targets of $CD8^+$ T cells responding to *L. monocytogenes* infection in C57BL/6 mice (Geginat et al., 2001; Platteel et al., 2016). The PlcA and PlcB antigens used in this study to develop a reverse immunology-based spliced epitope prediction method possess 317 residues and 292 residues, respectively. These two proteins lack known H-$2K^b$ presented epitopes. To identify potential spliced epitopes, we computed all possible 8-mer and 9-mer non-spliced and spliced peptides from the two antigens (Figure 1). Here, the peptide length was restricted to reduce the number of potential epitopes since 8-mer and 9-mer peptides represent the majority of the mouse MHC class I ligandome. The resulting database contained in total 1.56×10^6 sequences (Figures 2A and 2B). We then reduced the number of sequences by introducing further restrictions, which were based on previous studies. In particular, among the peptide candidates, we (1) set a maximal distance of 40 residues between the two splice reactants (i.e., the intervening sequence) and (2) excluded spliced peptides that were generated by binding of splice-reactants derived from two molecules of the same antigen (i.e., *trans* PCPS), as suggested by Dalet et al. (2010). Thus, only *cis*-spliced peptides, i.e., peptides generated from fragments of the same molecule, were included. This reduced database contained 4.67×10^5 entries for potential 8–9-mer spliced peptides and 1,188 entries for the potential 8–9-mer non-spliced peptides (Figures 2A and 2B). Because we were interested in antigenic peptides efficiently presented in the H-$2K^b$ cleft, we further reduced the database by selecting only those peptides that were predicted to bind H-$2K^b$ molecules with an $IC_{50} < 100$nM using the algorithm stabilized matrix method (SMM) (Peters and Sette, 2007) (Figures 1, 2C, and 2D). This selection step reduced the PlcA and PlcB candidate list to 989 spliced peptides and five non-spliced peptides. From these, we selected the 22 peptides with the lowest predicted IC_{50}, i.e., lower than 16 nM, which were all spliced peptides (Table 1; Figures S1 and S2), for further testing in ex vivo $CD8^+$ T cell recognition assays (Figure 1).

In summary, we applied several reduction steps in silico based on previously collected experimental evidence in order to obtain a candidate list of 22 predicted PlcA- and PlcB-spliced epitopes, starting from 1.56×10^6 potential spliced peptides. This led to progressive emergence of a peptide sequence pattern in the reduced databases, which included the known H-$2K^b$ anchor sites (Falk et al., 1991) (Figures 2E and 2F).

Specific $CD8^+$ T Cells Are Activated by PlcB-Derived and Proteasome-Generated Spliced Epitopes in *L. monocytogenes* Infection

To test the immunogenicity of the selected antigenic spliced epitope candidates, C57BL/6 mice were infected intravenously (i.v.) with 2,000 colony forming units (CFUs) *L. monocytogenes*. At day 7, the peak of the response (Busch et al., 1998), their splenocytes were isolated and frequencies of $CD8^+$ T cells producing interferon (IFN)-γ upon recognition of the spliced peptides were measured ex vivo, by intracellular cytokine staining and flow cytometry (Figure 3A). Two spliced PlcB epitope candidates, i.e., $PlcB_{189–191/163–167}$ and $PlcB_{189–192/164–167}$, as well as the known immunodominant non-spliced epitope $LLO_{296–304}$, stimulated IFN-γ production in a significant number of $CD8^+$ T cells (Figure 3B), indicating that these peptides are recognized by $CD8^+$ T cells responding to *L. monocytogenes* infection.

To confirm that the PlcB-derived spliced epitopes were generated by the proteasome, we performed in vitro digestions of the synthetic substrate $PlcB_{159–171/185–196}$ with 20S proteasomes purified from the spleens of *L. monocytogenes* infected or uninfected mice. The substrate sequences were derived from the original PlcB protein, although part of the intervening sequence ($PlcB_{172–184}$) was removed to facilitate the in vitro reaction as previously demonstrated (Dalet et al., 2010). MS analysis of the digests demonstrated the proteasome-mediated generation of the spliced epitopes $PlcB_{189–191/163–167}$ and $PlcB_{189–192/164–167}$ (Figure S3). By applying the quantitative method QME (quantification with minimal effort) to samples collected at different time intervals following in vitro digestion of $PlcB_{159–171/185–196}$, we measured the generation kinetics of the spliced epitopes

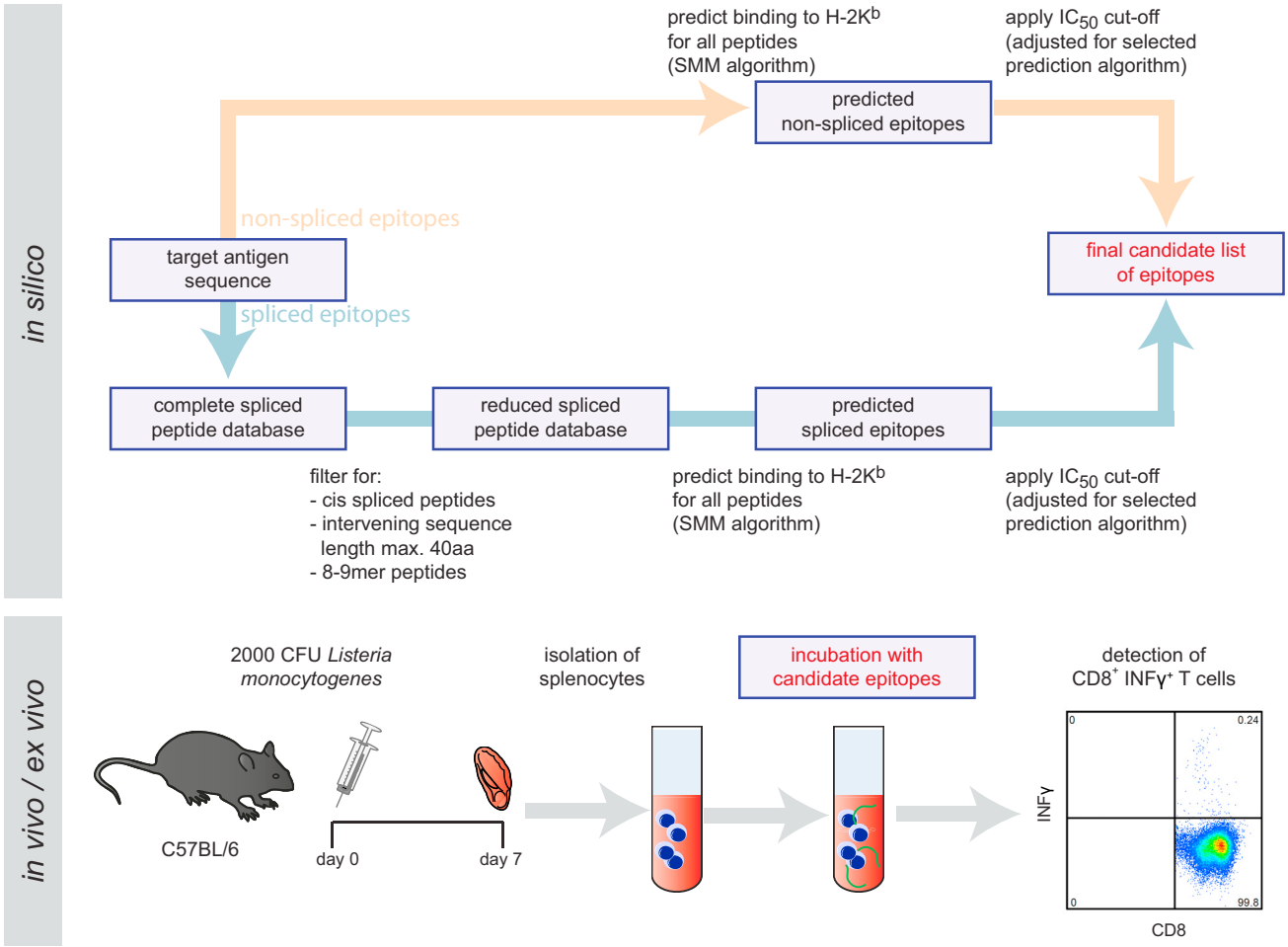

Figure 1. Reverse-Immunology Approach to Identifying Immunogenic Spliced Peptides In Vivo

The systematic identification of immunogenic peptides requires a combined in silico-in vitro approach. Illustrated is the identification of non-spliced peptides (pink arrows) and identification of spliced peptides (blue arrows). For the latter, we first computed the complete list of theoretically possible spliced peptides from a given antigen and reduced this step by step to a number of spliced peptides predicted to bind to the H-2K^b molecule. The final candidate list of epitopes then was tested ex vivo. C57BL/6 mice were infected with *L. monocytogenes*. After 7 days, the splenocytes were isolated and incubated with the spliced peptides from the final candidate list. Peptides that triggered IFN-γ production in CD8$^+$ T cells ex vivo (i.e., CD8$^+$ IFN-γ$^+$ T cells) were targeted by the *L. monocytogenes*-induced CD8$^+$ T cell response in vivo.

$PlcB_{189–191/163–167}$ and $PlcB_{189–192/164–167}$ (Figure S4). No remarkable differences in generation kinetics of the two spliced epitopes were detected between reactions carried out by proteasomes purified from either uninfected or infected mouse spleens.

Thus, we confirmed that the spliced epitopes $PlcB_{189–191/163–167}$ and $PlcB_{189–192/164–167}$ can be generated by the proteasome, both early in infection when proteasome composition has not yet been changed as result of the inflammatory milieu (see results with proteasomes of uninfected mouse spleens) and in later stages of infection.

CD8$^+$ T Cells Specific for the PlcB-Derived Spliced Epitopes Do Not Cross-React against Non-spliced Peptides in *L. monocytogenes* Infection

CD8$^+$ T cell responses to $PlcB_{189–191/163–167}$ and $PlcB_{189–192/164–167}$, detected ex vivo, may have been primed by non-spliced epitope variants rather than by the spliced epitopes. To rule out this possibility, we compared the frequencies of CD8$^+$ T cells in *L. monocytogenes* infected mouse spleens specific for the spliced epitopes $PlcB_{189–191/163–167}$ and $PlcB_{189–192/164–167}$, to the response elicited by the two non-spliced peptides $PlcB_{160–167}$ and $PlcB_{189–196}$, which shared part of the N or C terminus with the spliced epitopes (their generation kinetics are shown in Figure S4). Only the spliced epitopes were specifically recognized by CD8$^+$ T cells primed during *L. monocytogenes* infection (Figure 4A).

To further investigate the possibility that CD8$^+$ T cells, specific for the two spliced epitopes, were primed by Listeria-derived non-spliced peptides, we adapted an in silico analysis method, described by Calis et al. (2012). We first computed all spliced epitope-related peptides that could potentially prime cross-reactive CD8$^+$ T cells, due to T cell receptor (TCR) degeneracy. It has been shown that the amino acid residues at the anchor

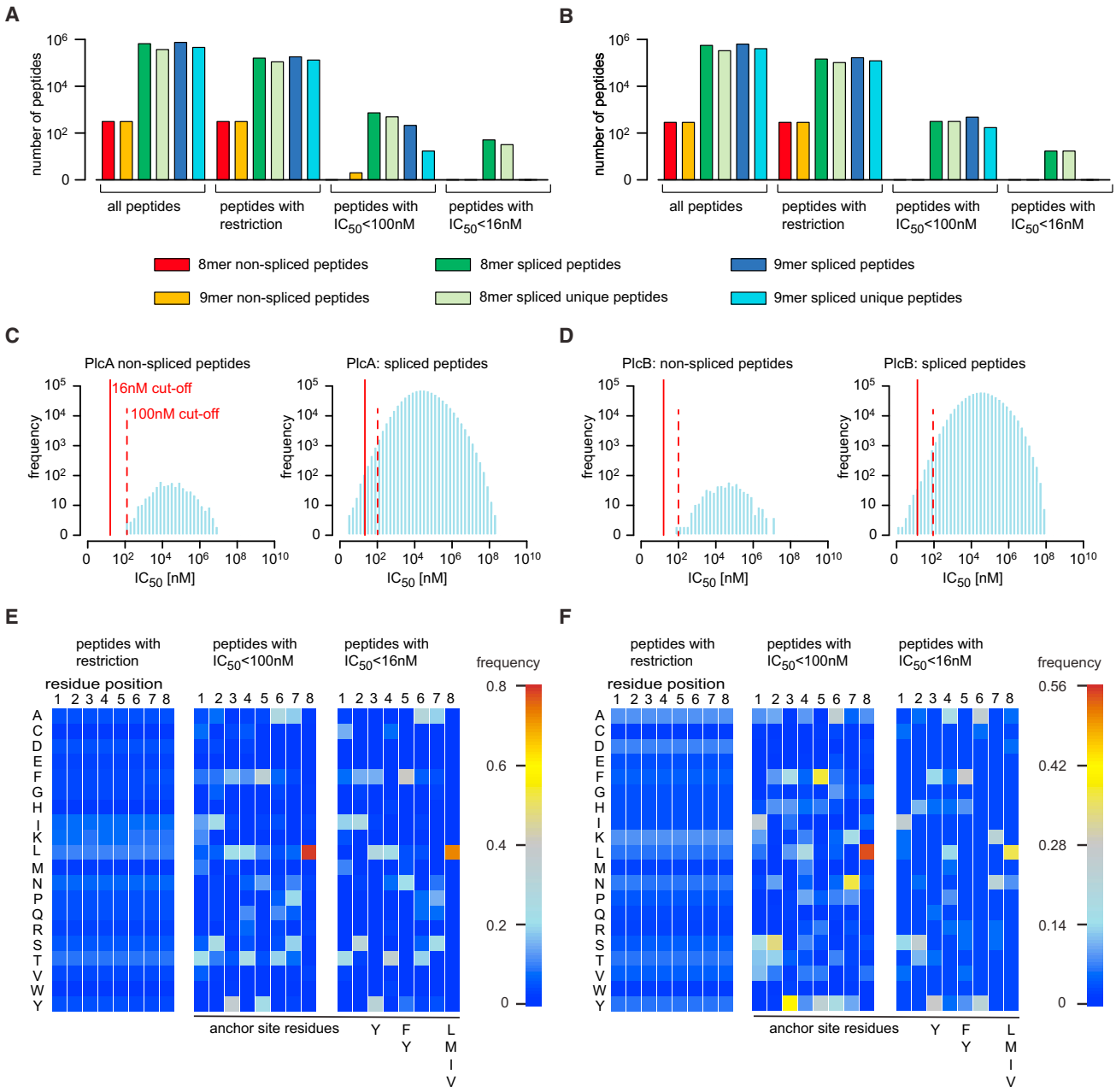

Figure 2. In Silico Identification of a Spliced Peptide Candidate List

(A and B) All possible 8-mer and 9-mer non-spliced and spliced peptides were computed for (A) PlcA and (B) PlcB. Shown is the reduction of the number of potential peptides based on the spliced peptide characteristics. It is often possible to produce the same sequence through different PCPS events from the same antigen, resulting in duplicate sequences. We therefore report both the total number of sequences and the number of unique sequences.

(C and D) For all 8-mer and 9-mer non-spliced peptides and for all 8-mer and 9-mer *cis*-spliced peptides with a maximum intervening sequence length of 40 amino acids the IC_{50} of binding to the H-2K^b molecule was predicted, shown as histograms in (C) PlcA and (D) PlcB. The IC_{50} cutoffs are indicated as red lines.

(E and F) The sequence profiles of 8-mer spliced peptides after each reduction step are shown in (E) PlcA and (F) PlcB. The frequencies represent the marginal probability distributions for each amino acid residue in the 8-mer spliced sequence. Below, the known anchor sites of the H-2K^b variants are denoted (Falk et al., 1991).

sites (3, 5, and 8 for the H2-K^b molecule) as well as the positions 1, 2, and 8 (for 9-mer) and 2, 3, and 8 (for 8-mer) are often irrelevant for efficient TCR recognition (Falk et al., 1991; Matsumura et al., 1992). We therefore computed all theoretical peptide sequences that followed the patterns ISXPXYKX, XXYPFYKX, and IXXPFYKX for the peptide PLCb$_{189–192/164–167}$ (ISYPFYKL)

Table 1. Predicted Spliced Epitope Candidates

Peptide[a]	Sequence	IC_{50} (nM)[b]	$T_{1/2}$ (hr)[c]
$LLO_{296–304}$[d]	VAYGRQVYL	8	1.4 ± 0.2
$PlcA_{70–72/92–96}$	MSYLYQQL	2.5	–
$PlcA_{70–73/93–96}$	MSYNYQQL	3.2	–
$PlcA_{262–266/273–275}$	TSLTFAAL	3.5	–
$PlcA_{262–267/285–286}$	TSLTFTNL	5.7	–
$PlcA_{262–268/254}$	TSLTFTPL	6.7	–
$PlcA_{70–72/57–61}$	MSYNLAAL	5.3	–
$PlcA_{262–266/284–286}$	TSLTFLNL	7.3	–
$PlcA_{112–114/92–96}$	KIYLYQQL	8.4	–
$PlcA_{19–23/59–61}$	CFFTFAAL	3.8	–
$PlcA_{19–23/56–58}$	CFFTFTNL	6.1	–
$PlcA_{19–23/50–52}$	CFFTFSAL	8.7	–
$PlcA_{19–24/57–58}$	CFFTFPNL	7.0	–
$PlcB_{189–191/163–167}$	ISYAFYKL	1.1	5.25 ± 0.92
$PlcB_{189–192/164–167}$	ISYPFYKL	1.9	4.05 ± 1.07
$PlcB_{171–173/163–167}$	IHYAFYKL	6.1	2.39 ± 0.71
$PlcB_{65–69/88–90}$	VNTHYANL	7.5	4.78 ± 1.69
$PlcB_{189–191/181–185}$	ISYMHANN	8.0	0.17 ± 0.12
$PlcB_{171–174/164–167}$	IHYYFYKL	8.1	1.66 ± 0.63
$PlcB_{251–255/270–272}$	KSYLVARL	8.6	3.13 ± 0.56
$PlcB_{118–121/137–140}$	STFLFANA	9.9	1.54 ± 0.25
$PlcB_{189–192/182–185}$	ISYPHANN	11.6	0.22 ± 0.14
$PlcB_{177–179/163–167}$	ISQAFYKL	15.4	1.43 ± 0.73
$PlcB_{160–167}$[e]	FDTAFYKL	2949	–[f]
$PlcB_{189–196}$[e]	ISYPPGYH	10840	–[f]
$PlcB_{189–191/163,164S–167S}$[g]	ISYASYKS	288	–
$PlcB_{189–192/164S–167S}$[g]	ISYPSYKS	473	–

[a]Spliced epitope candidates PlcA and PlcB antigens were predicted by applying the in silico computation method shown in Figure 1.
[b]The predicted IC_{50} for binding to the H-2K^b MHC class I molecule was calculated using SMM algorithm (Peters and Sette, 2007).
[c]The H-2K^b-peptide complex stability was empirically measured; mean half-life ($T_{1/2}$) and SD of two independent experiments are shown.
[d]The half-life of $LLO_{296–304}$ was in agreement with previous studies (Platteel et al., 2016).
[e]The two non-spliced peptides listed here were used as negative controls, to exclude potential cross-reactivity of spliced epitope-specific CD8$^+$ T cells.
[f]Peptides failed to stabilize H-2K^b molecules.
[g]In these spliced PlcB sequences, residue 164F and 167L were replaced for S residues, to decrease H-2K^b binding affinity.

and ISXAXYKX, XXYAFYKX, and IXXAFYKX for the peptide $PLCb_{189–191/163–167}$ (ISYAFYKL), where X could be any of the 20 amino acids. This resulted in 7,999 related peptides per candidate, which could theoretically prime CD8$^+$ T cells reactive also to the spliced epitope-specific, if any of these peptides were generated in vivo. However, none of these theoretical peptide sequences could be found in the *L. monocytogenes* non-spliced proteome (represented by 2,844 protein entries) (data not shown), thereby further suggesting that a hypothetical cross-reactivity of CD8$^+$ T cells against non-spliced PlcB-derived epitopes to the spliced epitopes, or the other way around, was unlikely.

To confirm that the specific CD8$^+$ T cell-mediated response toward the spliced epitopes in infected mice was the outcome of the infection, we compared the frequencies of spliced epitope-specific IFN-γ$^+$ CD8$^+$ T cells among splenocytes of infected mice to those of uninfected mice. For both the spliced ($PlcB_{189–191/163–167}$ and $PlcB_{189–192/164–167}$) and non-spliced ($LLO_{296–304}$) epitopes, we observed a significantly larger prevalence of IFN-γ$^+$ CD8$^+$ T cells in samples from infected mice compared to those from uninfected mice (Figure 4B), suggesting that the identified PlcB-derived spliced epitopes participate in the priming of CD8$^+$ T cell responses upon *L. monocytogenes* infection.

To prove that the identified spliced epitopes are processed from the PlcB protein and presented in vivo, EL4 cells (H-2K^b) were transduced with retroviral constructs expressing either full length PlcB or a mutated form of PlcB (PlcB-delta), in which the spliced epitopes' anchor residues were substituted for serine residues (F164S and L167S: $PlcB_{189–192/164–167}$ mutated to ISYPSYKS and $PlcB_{189–191/163–167}$ mutated to ISYASYKS), to interfere with H-2K^b binding (Table 1). These EL4 cells, as well as control EL4 cells transduced with an empty vector (Figure 5A) or EL4 cells expressing $LLO_{1–415}$, were co-cultured with purified CD8$^+$ splenocytes derived from PlcB-spliced epitope-responsive infected (Figure 3) or uninfected mice. Activation-induced IFN-γ release by CD8$^+$ T cells was quantified. As shown in Figure 5B, CD8$^+$ T cells derived from infected mice were activated by co-culture with EL4-LLO and EL4-PlcB cells, or by incubation with identified spliced epitopes (shown in Figure 3), but not by co-culture with PlcB-delta-expressing or mock transduced cells. Thus, disruption of spliced epitope presentation on H-2K^b molecules in EL4-PlcB-delta cells abrogated the ability of these cells to trigger IFN-γ production in PlcB-specific CD8$^+$ T cells derived from infected mice (Figure 5B). This indicates that these T cells recognize the spliced epitope sequences on EL4-PlcB cells and are not directed to peptides derived from another part of PlcB or from a different Listeria protein. As expected, CD8$^+$ splenocytes derived from non-infected mice failed to respond to any transduced EL4 cell line.

To exclude a theoretical cross-reaction of the spliced epitope-specific CD8$^+$ T cells against other spliced and non-spliced peptides generated by proteasomes from the epitope surrounding sequences, we analyzed $PlcB_{159–171/185–196}$ digestion products (Figure S3) by MS for the presence of other peptide products that carried one of the two residues substituted in the PlcB-delta, i.e., F164 or L167. Three non-spliced and ten spliced peptides containing PlcB F164 and/or L167 were identified (Table S1). We already demonstrated that the spliced epitopes $PlcB_{189–191/163–167}$ and $PlcB_{189–192/164–167}$ activated the CD8$^+$ T cells of infected mice, whereas the non-spliced peptides $PlcB_{160–167}$ did not (Figure 4A). Among the other peptide products, only the spliced peptide $PlcB_{187–191/164–167}$ was predicted to bind the H-2K^b complex with an IC_{50} lower than 100 nM, i.e., 73 nM, which is much larger than the IC_{50} of the overlapping spliced epitopes $PlcB_{189–191/163–167}$ and $PlcB_{189–192/164–167}$ and also than the IC_{50} of the spliced epitope candidates tested negative for recognition by CD8$^+$ T cells of *Listeria*-infected mice

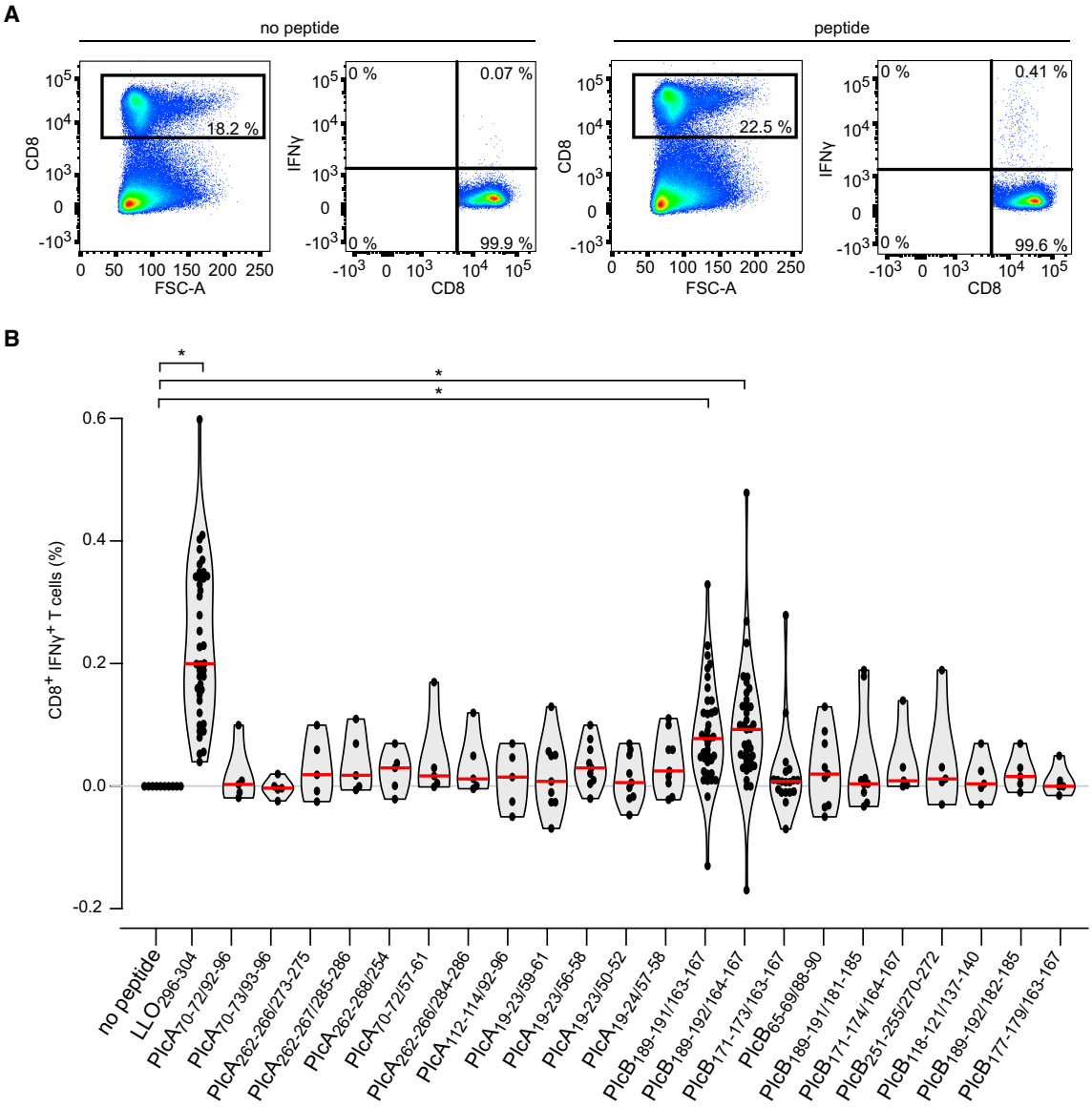

Figure 3. CD8⁺ T Cells from Infected Mice Specifically Recognize PlcB Spliced Epitopes

C57BL/6 mice were infected with *L. monocytogenes*, and 7 days later the frequency of CD8⁺ T cells specific for synthetic peptides among the splenocytes of infected mice was measured ex vivo by intracellular staining of IFN-γ in CD8⁺ T cells.

(A) Representative FACS plots of the staining in presence or absence of the target peptide $LLO_{296–304}$.

(B) Frequency of IFN-γ⁺ CD8⁺ T cells, upon ex vivo stimulation with the PlcA- or PlcB-spliced peptides and the non-spliced $LLO_{296–304}$ epitope, among splenocytes derived from infected mice (n = 5–43). Accumulated data of five independent experiments are shown, corrected for IFN-γ background measured in control samples incubated without peptide. The violin plots indicate the density of the measurements on each side, with all single mice indicated as dots. Red lines indicate the median of the measurements. Significant differences between the splenocytes incubated with or without the peptides are marked as * (ANOVA with Bonferroni and Welch's corrections; $LLO_{296–304}$, $PlcB_{189–191/163–167}$, and $PlcB_{189–192/164–167}$, $p < 0.001$).

(Figures S2 and 3 and see correlation between the frequency of the IFN-γ⁺ CD8⁺ T cells and the IC_{50} described below).

From these diverse control experiments, and the in vitro digestion experiments (Figure S4), we infer that cells expressing the *Listeria* PlcB protein generate the two PlcB-derived spliced epitopes in similar amounts (Figure S4) and present at least one of them to CD8⁺ T cells, triggering T cell activation. Given the absence of a CD8⁺ T cell response (1) toward the spliced PlcB epitopes in uninfected mice, (2) toward a non-spliced peptide sharing part of the spliced epitope sequence in infected mice, and (3) toward EL4 cells expressing a PlcB variant in which the MHC class I anchor sites of the two spliced epitopes are mutated, the possibility of cross-reactivity of the spliced PlcB epitope-specific CD8⁺ T cells is unlikely. This is further supported by the absence of other peptides produced by proteasomes and predicted to efficiently bind to H-2K^b molecules.

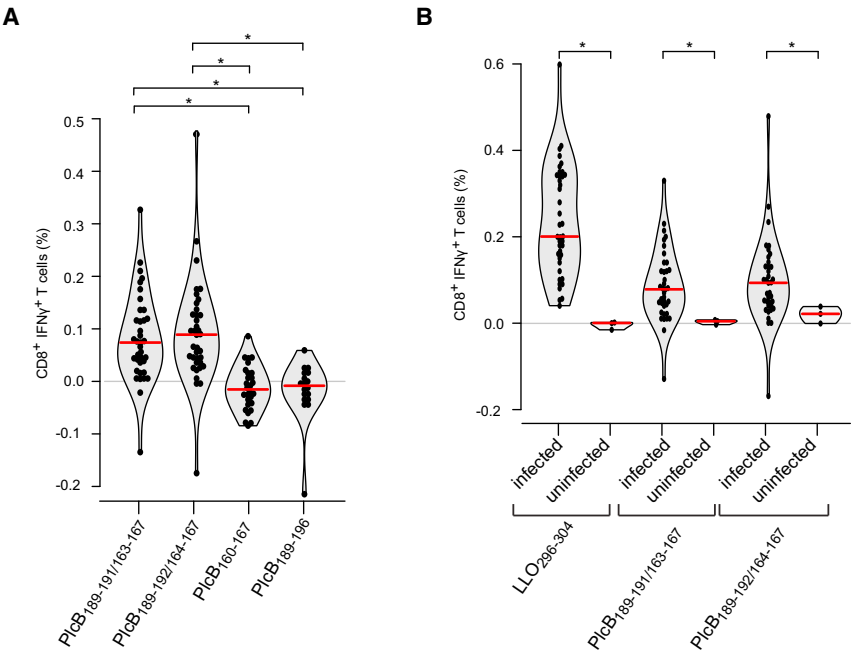

Figure 4. PlcB-Spliced Epitope-Specific CD8$^+$ T Cells Are Not Cross-Reactive to PlcB Non-spliced Peptides and Are Not Activated in Uninfected Mice

(A) Frequency of IFN-γ^+ CD8$^+$ T cells, upon ex vivo stimulation with the $PlcB_{189–191/163–167}$- and $PlcB_{189–192/164–167}$-spliced epitopes and the $PlcB_{160–167}$ and $PlcB_{189–196}$ non-spliced peptides, among splenocytes derived from *L. monocytogenes* infected mice (n = 18–37) is shown. Accumulated data of five independent experiments are shown per peptide corrected for IFN-γ background level as measured in control samples that were incubated without peptide. The violin plots indicate the density of the measurements on each side, with all single mice indicated as dots. Red lines indicate the median of the measurements. Significant differences between the splenocytes incubated with spliced epitopes and non-spliced peptides are marked as * (ANOVA upon Bonferroni and Welch's corrections; $PlcB_{189–191/163–167}$ or $PlcB_{189–192/164–167}$ versus $PlcB_{160–167}$ or $PlcB_{189–196}$, $p < 0.001$).

(B) Frequency of IFN-γ^+ CD8$^+$ T cells, upon ex vivo stimulation with $LLO_{296–304}$, $PlcB_{189–191/163–167}$, and $PlcB_{189–192/164–167}$, among splenocytes derived from infected (n = 37–40) or uninfected (n = 3) mice. Accumulated data of five independent experiments are shown. Significant differences between infected and uninfected mice are marked as * (t-student with Welch's correction; $LLO_{296–304}$, and $PlcB_{189–191/163–167}$, $p < 0.001$; $PlcB_{189–192/164–167}$, $p = 0.001$).

Measured H-2K^b-Spliced Peptide Stability and the Predicted Binding Affinity Correlate with the Relative Frequency of Specific CD8$^+$ T Cells in Infected Mice

During the development of our in silico strategy for selecting the best peptide candidates for this study, we assumed, based on earlier studies (Sijts and Pamer, 1997; van der Burg et al., 1996; Watson et al., 2012), a correlation between the predicted IC_{50} (i.e., H-2K^b binding affinity) and the recognition of peptides by specific CD8$^+$ T cells. Therefore, we restricted the list of spliced peptides that might be recognized during *L. monocytogenes* infection by their predicted IC_{50}. The validity of this approach was evaluated on the results of the ex vivo stimulation of splenocytes derived from infected mice with the PlcB-spliced peptides (Figure 6). In agreement with our assumption, we observed a significant inverse correlation between the predicted IC_{50} of the spliced peptides and the specific response (measured as frequency of IFN-γ^+ CD8$^+$ T cells ex vivo) in infected mice (Figure 6A; Table 1).

As proof of principle, we experimentally measured another parameter depicting the affinity between MHC class I and peptide, i.e., the stability of H-2K^b-peptide complexes at the cell surface of RMA-S cells (Figure 6B). Five out of ten spliced PlcB epitope candidates tested, including $PlcB_{189–191/163–167}$ and $PlcB_{189–192/164–167}$, upregulated H-2K^b levels on RMA-S cells (Figure 6C, left panel), indicating that these peptides bound to and stabilized RMA-S-expressed H-2K^b molecules. The other spliced epitope candidates tested (Figure 6C, right panel) as well as the non-spliced peptides $PlcB_{160–167}$ and $PlcB_{189–196}$ (data not shown), only weakly upregulated or failed to upregulate H-2K^b on RMA-S cells. This difference in peptide binding capacity was illustrated by the half-lives that we computed based on chase analyses of peptide-pulsed RMA-S cells (Table 1), which varied from 5.25 hr for H-2K^b complexed with "strong" binders to 0.17 hr for weak binders. Of note, the two identified spliced epitopes $PlcB_{189–191/163–167}$ and $PlcB_{189–192/164–167}$ were among the three highest affinity H-2K^b binders (Table 1), with computed half-lives exceeding these of H-2K^b molecules bound to the control epitope $LLO_{296–304}$. Comparing the data for all spliced peptides tested, we found a significant inverse correlation between the predicted IC_{50} and the measured half-lives of H-2K^b-peptide complexes at the cell surface (Figure 6D). Accordingly, we also found a significant direct correlation between the half-lives of H-2K^b-peptide complexes and the relative frequency of IFN-γ^+ CD8$^+$ T cells among infected mouse' splenocytes for the spliced peptides derived from PlcB (Figure 6E). Thus, selection of spliced epitope candidates based on predicted IC_{50} is a valid approach for focusing ex vivo analyses on the most promising epitope candidates.

DISCUSSION

We here present a multi-level spliced epitope identification approach that will be instrumental in uncovering the role of PCPS in immune recognition, both of pathogen-derived and self-antigens. Application of this approach enabled us to gain insight into the contribution of PCPS to MHC class I antigen processing. Focusing on two *L. monocytogenes* proteins as model antigens, we show that PCPS generates two overlapping spliced epitopes that participate in CD8$^+$ T cell priming following infection. The precise contribution of the two respective peptides to CD8$^+$ T cell activation will be unraveled in future experiments aimed at examining the MHC class I presentation kinetics of the spliced epitopes in relation to each other as well as to other, non-spliced Listeria epitopes.

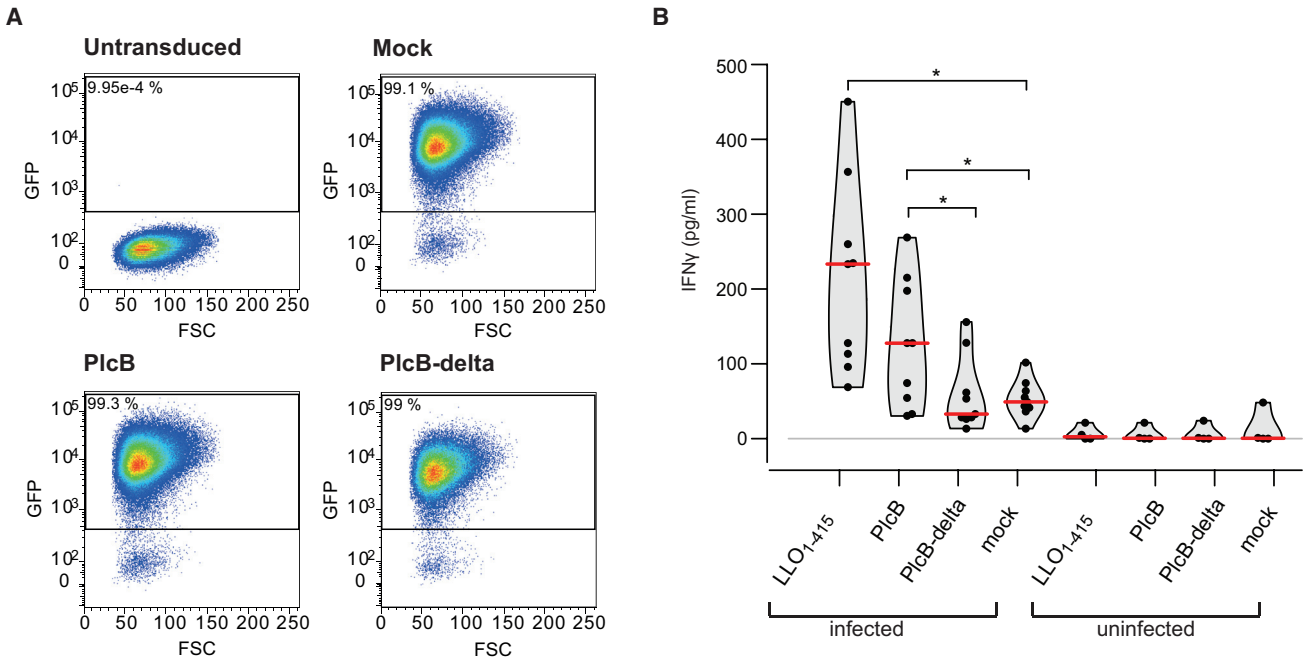

Figure 5. Identified PlcB-Spliced Epitopes Are Processed and Presented by EL4 Cells Expressing the *L. monocytogenes*-Derived PlcB Protein

(A) Representative plot of GFP expression by EL4 cells transduced with retroviral vectors carrying the GFP gene and the target constructs PlcB and PlcB-delta. Mock: empty-vector-transduced cells.

(B) Purified $CD8^+$ splenocytes of infected and uninfected mice were co-cultured with EL4 cells transduced with $LLO_{1–415}$, PlcB, PlcB-delta or the empty vector (mock). After 48 hr the supernatants were collected and IFN-γ was quantified (pg/mL). The data of one experiment with a pool of ten animals, representative of three independent experiments (total n = 48), performed with thawed and fresh $CD8^+$ splenocytes, are shown (red bars: means). Significant differences in IFN-γ release by splenocytes of infected mice co-cultured with LLO versus mock cells ($p = 0.0025$), PlcB versus mock cells ($p = 0.0187$), and PlcB versus PlcB-delta cells ($p = 0.0328$) are marked as * (t-student with Welch's correction).

The method developed for this study to identify spliced epitope candidates uses an in silico-guided approach for the identification of spliced peptides, combined with experimental outcomes and the SMM prediction algorithm. As part of this approach, in silico-predicted epitope candidates are selected based on their low predicted IC_{50}, which showed to be the right approach since we observed a correlation between predicted IC_{50} (and H-$2K^b$-peptide complex stability) and the expansion of specific $CD8^+$ T cells during infection, in agreement with earlier published works (Sijts and Pamer, 1997; van der Burg et al., 1996; Watson et al., 2012).

The demonstration that proteasome-generated spliced epitopes trigger a specific $CD8^+$ T cell response during *L. monocytogenes* infection in mice could represent a mile stone in the investigation of T cell immunity against pathogens. The ability of PCPS to expand the epitope variety could be a key means of the immune system to tackle the high mutation frequency and therewith the escape mechanisms of some pathogens. The enormous number of potential combinations of spliced peptides derived from an antigen could also be a means for allowing the immune system to target antigens with few or none non-spliced antigenic peptides that could be effectively presented by the MHC class I molecules of a person.

Thus, the so-far neglected possibilities for epitopes generated by PCPS may be a tremendous asset for vaccination approaches focusing on single pathogen-derived proteins. To illustrate this, we performed a preliminary in silico analysis to identify PlcA and PlcB epitope candidates for the most frequent human MHC class I haplotypes (Figures S5 and S6). We calculated that the number of potential spliced peptides predicted to bind with high affinity to the most frequent HLA-A or HLA-B variants largely exceeds that of the non-spliced peptides. Thus, no non-spliced epitope candidates with a predicted IC_{50} below 100 nM were found in PlcB or in PlcA in combination with HLA-A*01:01, HLA-A*03:01, HLA-B*44:02, or HLA-B*44:03, while four and three non-spliced candidates were predicted for the PlcA antigen in combination with HLA-A*02:01 and HLA-B*07:02, respectively. In contrast, there are hundreds of potential spliced epitopes for both antigens predicted to bind to each of the investigated MHC class I haplotypes (Figures S5 and S6).

In conclusion, we suggest that spliced peptides might provide immunological targets as well as a key means by which the immune system tackles pathogens.

EXPERIMENTAL PROCEDURES

In Silico Generation of Spliced Peptide Target List

Given the PlcA (AEO05212.1) or PlcB (AEO05216.1) sequences, we first computed all potential non-spliced and spliced peptides of length L = 8 and

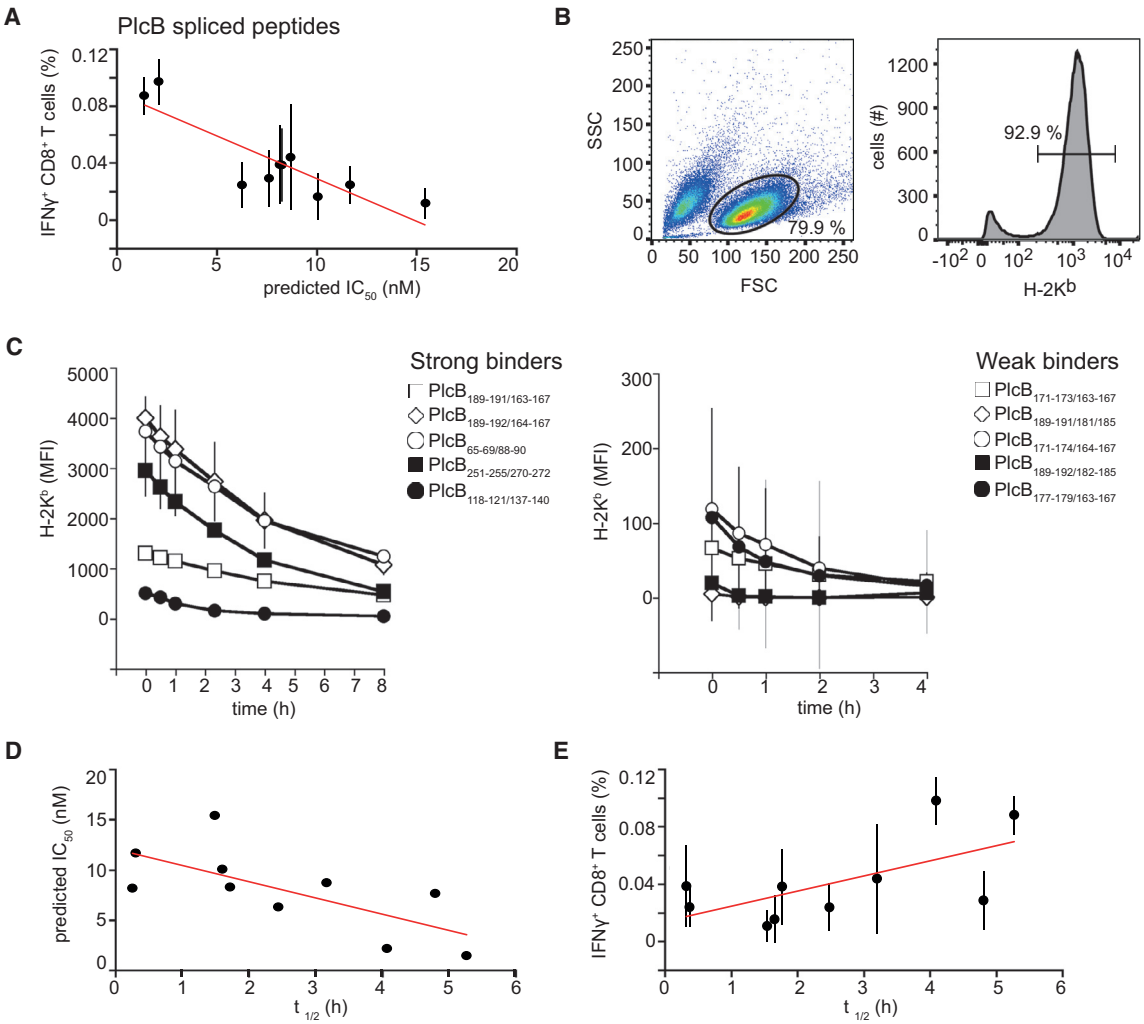

Figure 6. Correlation between Predicted IC_{50}, H-2K^b-Peptide Stability, and Frequency of Specific CD8$^+$ T Cells in Infected Mice

(A) Correlation between the predicted IC_{50} of PlcB-spliced peptides and the frequency of IFN-γ^+ CD8$^+$ T cells specific for the peptides among splenocytes derived from *L. monocytogenes* infected mice (for all PlcB peptides tested on five to 37 mice). There is a significant inverse correlation (Spearman correlation test $p < 0.001$, C value = −0.559). Values are the mean and bars the SEM of tested mice for each peptide (n = 5–37). IC_{50} of the peptides for the H-2K^b complex was predicted by the SMM algorithm (Peters and Sette, 2007).

(B) H-2K^b-peptide stability was measured with RMA-S cells incubated with synthetic peptides and chased in the absence of peptide. At different time points the remaining H-2K^b-peptide complexes were measured using FACS and measured in MFI (mean fluorescence index).

(C) The stability of the H-2K^b complexes bound to each PlcB-spliced peptide is shown. Peptides were divided in strong binders (with MFI > 500 at t = 0; left panel) or weak binders (with MFI < 200 at t = 0; right panel). Incubation without peptide resulted in a background MFI level of ~40. Values are the mean MFI ± SD of two independent experiments.

(D) Correlation between the predicted IC_{50} of the PlcB-spliced peptides (n = 10) and the H-2K^b-peptide half-life at the cells surface is shown. Values are the mean of two independent experiments. There is a significant inverse correlation (Spearman correlation test $p = 0.022$, C value = −0.709).

(E) Correlation between the H-2K^b-peptide stability and the frequency of IFN-γ^+ CD8$^+$ T cells responsive against the spliced peptides among splenocytes derived from infected mice (for all peptides tested on five to 37 mice). There is a significant correlation (Spearman correlation test $p < 0.001$, C value = 0.498). Values are the mean and bars the SEM of mice tested for each peptide (n = 5–37).

L = 9, resulting in N peptides, denoted as [n-p1]/[p2-c], where N can be obtained via Equation 1 derived from Liepe et al. (2010).

$$N = \sum_{L=8}^{9} \sum_{n=1}^{S} \sum_{p1=n}^{n+L-2} \sum_{p2}^{S-L+p1-n+1} 1, \qquad \text{(Equation 1)}$$

where S is the length of the parental antigen (PlcA and PlcB, respectively). This list was then reduced by excluding all spliced peptides generated through *trans* PCPS. This means that for a given spliced peptide denoted as [n-p1]/[p2-c] all peptides with p1 < p2 (for PCPS in same order as in parental antigen) or c < n (for PCPS in reverse order compared to the parental antigen) are maintained in the reduced database). We next removed all peptides with intervening sequence length l larger than 40 amino acids, where l is defined as l = p2-p1-1 for splicing in normal order, and l = c-n-1 for splicing in reverse order. For all remaining 8- and 9-mer spliced peptides, we computed in silico the IC_{50} as a measure for binding strength to the murine H-2K^b or the human HLA-A*01:01, HLA-A*02:01, HLA-A*03:01, HLA-B*07:02, HLA-B*44:02, and

HLA-B*44:03 haplotypes using the offline version of the SMM algorithm (Peters and Sette, 2007). We considered all spliced peptides with predicted IC_{50} <100 nM and a further IC_{50} cutoff of 16 nM.

Peptide Synthesis and 20S Proteasome Purification

The $PlcB_{159–171/185–196}$ (KFDTAFYKLGLAINFTAISYPPGYH) polypeptide substrate and all non-spliced and spliced PlcA and PlcB peptides were synthesized using Fmoc solid phase chemistry. 20S proteasomes were purified from five pooled spleens of C57BL/6 mice infected or uninfected by *L. monocytogenes* (Platteel et al., 2016). The purity of the proteasome preparation is shown in Figure S7. The differences in proteasome subunit composition were described previously (Platteel et al., 2016).

Identification and Quantification of Peptide Products from In Vitro Digestions by Proteasomes

$PlcB_{159–171/185–196}$ (20 μM) was digested by 2 μg 20S proteasomes in 100 μL TEAD buffer (Tris 20 mM, EDTA 1 mM, NaN_3 1 mM, DTT 1 mM [pH 7.2]) over time, at 37°C. Identification of the polypeptide digestion products was performed by liquid-chromatography mass spectrometry (LC-MS) analyses: 15-μL digested samples were analyzed directly by nanoscale LC-MS/MS using an Ultimate 3000 and LTQ Orbitrap XL mass spectrometer (Thermo Fisher Scientific). The system comprises a 5-mm × 300-μm, 100-Å trapping column (PepMap C18, 5 μm; Dionex) and a PicoChip analytical column (Reprosil-pur; 3 μm; New Objective). The mobile phase (A) was 0.1% (v/v) formic acid in water and (B) was 80:20 (v/v) acetonitrile/water containing 0.1% (v/v) formic acid. Elution was carried out using a gradient 15%–50% B in 35 min with a flow rate of 300 nL/min. Full MS spectra (m/z 300–2,000) were acquired in an Orbitrap instrument at a resolution of 60,000 (full width at half maximum [FWHM]). At first, the most abundant precursor ion was selected for either data-dependent collision-induced dissociation (CID) fragmentation with parent list (1^+, 2^+ charge state included). Fragment ions were detected in an Ion Trap instrument. Dynamic exclusion was enabled with a repeat count of 2- and 60-s exclusion duration. Additional, the theoretically calculated precursor ions of the expected spliced peptides were pre-elected for two Orbitrap CID (m/z 350–2,000) and higher energy collisional dissociation (HCD; m/z 100–1500) fragmentation scans. The maximum ion accumulation time for MS scans was set to 200 ms and for MS/MS scans to 500 ms. Background ions at m/z 391.2843 and 445.1200 act as lock mass. Peptides were identified by PD1.4 software (Thermo Fisher Scientific) based on their merged tandem mass spectra (MS/MS) of CID and HCD. In addition, for spliced peptides we compared the retention time and the merged MS/MS of CID and HCD with the fragmentation pattern of their synthetic counterparts. The database used for the LC-MS/MS analyses was generated by applying the SpliceMet's ProteaJ algorithm thereby allowing the identification of non-spliced and spliced peptides (Liepe et al., 2010).

The polypeptide digestion kinetics were analyzed with the ESI-ion trap instrument DECA XP MAX (Thermo Fisher Scientific) as described (Liepe et al., 2010). The quantification of peptides produced in the in vitro digestion kinetics was carried out by applying the QME method to the LC-MS analyses (Mishto et al., 2012). QME estimates the absolute content of spliced and non-spliced peptide products based on their MS peak area measured in the digestion probe. The QME algorithm parameters were empirically computed in our previous study (Mishto et al., 2012) and here applied.

Cell Culture

RMA-S cells were cultured in IMDM (Invitrogen Life Technologies), supplemented with 10% fetal calf serum (FCS; LONZA), 2 mM L-glutamine, 30 μM 2-ME, and 100 U/mL penicillin/streptomycin. 293T cells were maintained in DMEM (Invitrogen Life Technologies) supplemented with 10% FCS and penicillin/streptomycin. Transduced EL4 cells were cultured in RPMI (Invitrogen Life Technologies), supplemented with 10% FCS, 2 mM L-glutamine, 30 μM 2-ME, penicillin/streptomycin, and 5 μg/mL puromycin (Sigma-Aldrich) as appropriate.

MHC Class I Peptide Stability Assays

RMA-S off rate assays were performed as described (Deol et al., 2007). In short, TAP-deficient RMA-S cells were incubated overnight (o/n) in the presence or absence of 100 μM synthetic peptide, at 37°C. Cells were harvested, washed three times with PBS, and chased in the absence of peptide, at 37°C, stained for H-$2K^b$ class I expression with a conformation-sensitive, biotin-conjugated mouse antibody (Ab) (AF6-88.5; BD Bioscience) and PE-conjugated SA (eBioscience) and analyzed using fluorescence-activated cell sorting (FACS) Canto II (BD Bioscience) and FlowJo software (Tree Star). The $T_{1/2}$ of the H-$2K^b$-peptide complex at the cell surface was computed as described (Textoris-Taube et al., 2015), based on the mean fluorescence levels of peptide-pulsed cells corrected for background levels from cells that were not incubated with peptide.

Retroviral Transduction of EL4 Cells

$LLO_{1–415}$ was amplified from *L. monocytogenes* 10403S using forward primer AGATCTGTGAAACCCATGAAAAAAATAATGCTAG and reverse primer TTAATCTGTATAAGCTTTTGAAGTTGTTTC. The product was verified by sequencing and cloned into a pMSCV_IRES_GFP vector (Addgene). Synthetic DNA sequences of PlcB and PlcB-delta (with the substitutions F164S and L167S) were purchased (Geneart Invitrogen) and cloned into pMSCV-Puro-IRES-GFP. pMSCV constructs and pCl-10A1, encoding the envelope proteins, were transfected into 293T cells using Lipofectamine 2000 reagent (Thermo Fisher Scientific) as instructed. After 24 hr, the medium was removed and cells were co-cultured with EL4 cells, added in 10 mL medium, for 48 hr at 37°C. EL4 cells were then harvested, resuspended in 10 mL DMEM medium without (LLO-transduced cells) or with puromycin (PlcB, PlcB-delta and mock cells). Expression of the constructs was verified by GFP expression using FACS and found to be ~99% (Figure 5A) for PlcB, PlcB-delta, and mock cells. LLO-expressing cells were sorted by FACS twice, which resulted in expression levels of ~20%.

Mice and Infection

L. monocytogenes strain 10403S was grown in brain-heart infusion medium (Sigma-Aldrich) and harvested while in log phase. C57BL/6 mice were purchased from Charles River. For infection, 6 to 8-week-old female mice were inoculated intravenously in the tail vain with 2000 bacteria (0.1 LD50) in 200 μL PBS. All animal experiments were approved by the Animal Ethics Committee from Utrecht University (DEC 2014.II.11.081 and DEC 2014.II.01.003).

Intracellular IFN-γ Staining

Erythrocyte-depleted single spleen cell suspensions were prepared and 0.5×10^6 splenocytes were incubated with or without 1 μg/mL synthetic peptide for 6 hr in 1 mL RPMI medium, containing 50 μg/mL gentamycin (Gibco), and 10 μM monensin (eBioscience), at 37°C. Subsequently, cells were stained with an antigen-presenting cell (APC)-conjugated anti-mouse CD8 antibody (53-6.7; eBioscience) in the presence of anti-mouse CD16/CD32 antibody (clone 2.4G2; made in house). Cells were fixed with 2% paraformaldehyde and then stained with phycoerythrin (PE)-conjugated anti-mouse IFN-γ antibody (XMG1.2; eBioscience) in the presence of 0.5% saponin and analyzed on a FACS Canto II (BD Biosciences) using FlowJo software (Tree Star). Percentages of specific IFN-γ^+ $CD8^+$ splenocytes were calculated by subtracting the background IFN-γ^+ $CD8^+$ level of splenocytes incubated without peptide per individual mouse.

Detection of IFN-γ Release

$CD8^+$ splenocytes were enriched by negative selection for CD4 (GK1.5), B220 (RA3-6B2), CD11b (M1/70), and MHCII (M5/114)-expressing cells using Dynal beads (Invitrogen). 4×10^5 $CD8^+$ cells (purity ~80%) were co-cultured with 2×10^5 transduced EL4 cells for 48 hr, and supernatants were then collected for analysis in a monoplex IFN-γ assay using the Magpix (Luminex XMAP) system, as instructed. Briefly, supernatant were incubated o/n with magnetic IFN-γ capture beads (clone AN-18), in 96-well flat-bottomed plates (Greiner bio-one, 655096). Captured IFN-γ was detected with biotin-conjugated anti-IFN-γ mAb (clone XMG1.2) and Streptavidin-PE. Cytokine concentrations in the tested samples were calculated from a standard curve generated with rIFN-γ and MFI data were analyzed using a 5-parameter logistic method (xPONENT software, Luminex).

Statistical Analysis

Data were tested for normality distribution and homoscedasticity by Kolmogorov-Smirnov, Shapiro-Wilk, and Levene tests. To test for significant differences between $CD8^+$ T cell responses to different epitope candidates, we applied an unpaired ANOVA test with Bonferroni post hoc correction for multiple comparisons and Welch's correction. To compare frequencies of peptide-specific $CD8^+$ T cells between infected and uninfected mice, we applied an unpaired t test with Welch's correction. The same test was performed in Figure 5 to compare INF-γ release by $CD8^+$ T cells toward EL4 cells expressing LLO, PlcB, PlcB-delta as compared to those expressing the empty vector (mock). For the correlations, we applied a Spearman test. $p < 0.05$ was considered to be significant.

ACCESSION NUMBERS

The FACS files and mass spectrometry RAW files reported in this paper are available in Mendeley Data at DOI http://dx.doi.org/10.17632/983y6nncrx.1.

SUPPLEMENTAL INFORMATION

Supplemental Information includes seven figures and one table and can be found with this article online at http://dx.doi.org/10.1016/j.celrep.2017.07.026.

AUTHOR CONTRIBUTIONS

Conceptualization, A.C.M.P., J.L., M.M., and A.J.A.M.S.; Investigation, A.C.M.P., J.L, M.M., K.T.-T., H.H.S., R.C., C.K., and P.H.; Writing, Review, & Editing, A.C.M.P., J.L., M.M., A.J.A.M.S., and P.M.K.; Funding Acquisition, A.J.A.M.S. and P.M.K.; Resources, A.J.A.M.S. and P.M.K.; Supervision, M.M., A.J.A.M.S., and P.M.K.

ACKNOWLEDGMENTS

Support was by European Union's Seventh Framework Programme (FP7/2007-2013) grant no. 280873: ADITEC to A.J.A.M.S., Berlin Institute of Health (BIH, CRG1-TP1) and Einstein Stiftung Berlin (A2013-174) to P.M.K., and NC3Rs through a David Sainsbury Fellowship to J.L. (NC/K001949/1). We thank P. Kunert and B. Brecht-Jachan (Charité Berlin) for technical assistance. We thank the Shared Facility Mass Spectrometry of the Charité for support in data acquisition.

Received: October 31, 2016
Revised: June 26, 2017
Accepted: July 12, 2017
Published: August 1, 2017

REFERENCES

Arciniega, M., Beck, P., Lange, O.F., Groll, M., and Huber, R. (2014). Differential global structural changes in the core particle of yeast and mouse proteasome induced by ligand binding. Proc. Natl. Acad. Sci. USA *111*, 9479–9484.

Bielecki, J., Youngman, P., Connelly, P., and Portnoy, D.A. (1990). Bacillus subtilis expressing a haemolysin gene from Listeria monocytogenes can grow in mammalian cells. Nature *345*, 175–176.

Busch, D.H., Pilip, I.M., Vijh, S., and Pamer, E.G. (1998). Coordinate regulation of complex T cell populations responding to bacterial infection. Immunity *8*, 353–362.

Calis, J.J., de Boer, R.J., and Keşmir, C. (2012). Degenerate T-cell recognition of peptides on MHC molecules creates large holes in the T-cell repertoire. PLoS Comput. Biol. *8*, e1002412.

Cascio, P., Hilton, C., Kisselev, A.F., Rock, K.L., and Goldberg, A.L. (2001). 26S proteasomes and immunoproteasomes produce mainly N-extended versions of an antigenic peptide. EMBO J. *20*, 2357–2366.

Dalet, A., Vigneron, N., Stroobant, V., Hanada, K., and Van den Eynde, B.J. (2010). Splicing of distant peptide fragments occurs in the proteasome by transpeptidation and produces the spliced antigenic peptide derived from fibroblast growth factor-5. J. Immunol. *184*, 3016–3024.

Dalet, A., Robbins, P.F., Stroobant, V., Vigneron, N., Li, Y.F., El-Gamil, M., Hanada, K., Yang, J.C., Rosenberg, S.A., and Van den Eynde, B.J. (2011). An antigenic peptide produced by reverse splicing and double asparagine deamidation. Proc. Natl. Acad. Sci. USA *108*, E323–E331.

Deol, P., Zaiss, D.M.W., Monaco, J.J., and Sijts, A.J.A.M. (2007). Rates of processing determine the immunogenicity of immunoproteasome-generated epitopes. J. Immunol. *178*, 7557–7562.

Ebstein, F., Textoris-Taube, K., Keller, C., Golnik, R., Vigneron, N., Van den Eynde, B.J., Schuler-Thurner, B., Schadendorf, D., Lorenz, F.K., Uckert, W., et al. (2016). Proteasomes generate spliced epitopes by two different mechanisms and as efficiently as non-spliced epitopes. Sci Rep. *6*, 24032.

Falk, K., Rötzschke, O., Stevanović, S., Jung, G., and Rammensee, H.G. (1991). Allele-specific motifs revealed by sequencing of self-peptides eluted from MHC molecules. Nature *351*, 290–296.

Geginat, G., Schenk, S., Skoberne, M., Goebel, W., and Hof, H. (2001). A novel approach of direct ex vivo epitope mapping identifies dominant and subdominant CD4 and CD8 T cell epitopes from Listeria monocytogenes. J. Immunol. *166*, 1877–1884.

Groettrup, M., Kirk, C.J., and Basler, M. (2010). Proteasomes in immune cells: More than peptide producers? Nat. Rev. Immunol. *10*, 73–78.

Hanada, K., Yewdell, J.W., and Yang, J.C. (2004). Immune recognition of a human renal cancer antigen through post-translational protein splicing. Nature *427*, 252–256.

Liepe, J., Mishto, M., Textoris-Taube, K., Janek, K., Keller, C., Henklein, P., Kloetzel, P.M., and Zaikin, A. (2010). The 20S proteasome splicing activity discovered by SpliceMet. PLoS Comput. Biol. *6*, e1000830.

Liepe, J., Holzhütter, H.G., Bellavista, E., Kloetzel, P.M., Stumpf, M.P.H., and Mishto, M. (2015). Quantitative time-resolved analysis reveals intricate, differential regulation of standard- and immuno-proteasomes. eLife *4*, e07545.

Liepe, J., Marino, F., Sidney, J., Jeko, A., Bunting, D.E., Sette, A., Kloetzel, P.M., Stumpf, M.P., Heck, A.J., and Mishto, M. (2016). A large fraction of HLA class I ligands are proteasome-generated spliced peptides. Science *354*, 354–358.

Matsumura, M., Fremont, D.H., Peterson, P.A., and Wilson, I.A. (1992). Emerging principles for the recognition of peptide antigens by MHC class I molecules. Science *257*, 927–934.

Michaux, A., Larrieu, P., Stroobant, V., Fonteneau, J.F., Jotereau, F., Van den Eynde, B.J., Moreau-Aubry, A., and Vigneron, N. (2014). A spliced antigenic peptide comprising a single spliced amino acid is produced in the proteasome by reverse splicing of a longer peptide fragment followed by trimming. J. Immunol. *192*, 1962–1971.

Mishto, M., Goede, A., Taube, K.T., Keller, C., Janek, K., Henklein, P., Niewienda, A., Kloss, A., Gohlke, S., Dahlmann, B., et al. (2012). Driving forces of proteasome-catalyzed peptide splicing in yeast and humans. Mol. Cell. Proteomics *11*, 1008–1023.

Mishto, M., Liepe, J., Textoris-Taube, K., Keller, C., Henklein, P., Weberruß, M., Dahlmann, B., Enenkel, C., Voigt, A., Kuckelkorn, U., et al. (2014). Proteasome isoforms exhibit only quantitative differences in cleavage and epitope generation. Eur. J. Immunol. *44*, 3508–3521.

Pamer, E.G. (2004). Immune responses to Listeria monocytogenes. Nat. Rev. Immunol. *4*, 812–823.

Peters, B., and Sette, A. (2007). Integrating epitope data into the emerging web of biomedical knowledge resources. Nat. Rev. Immunol. *7*, 485–490.

Platteel, A.C.M., Mishto, M., Textoris-Taube, K., Keller, C., Liepe, J., Busch, D.H., Kloetzel, P.M., and Sijts, A.J.A.M. (2016). CD8(+) T cells of Listeria monocytogenes-infected mice recognize both linear and spliced proteasome products. Eur. J. Immunol. *46*, 1109–1118.

Portnoy, D.A., Chakraborty, T., Goebel, W., and Cossart, P. (1992). Molecular determinants of Listeria monocytogenes pathogenesis. Infect. Immun. *60*, 1263–1267.

Rock, K.L., Gramm, C., Rothstein, L., Clark, K., Stein, R., Dick, L., Hwang, D., and Goldberg, A.L. (1994). Inhibitors of the proteasome block the degradation of most cell proteins and the generation of peptides presented on MHC class I molecules. Cell *78*, 761–771.

Ruschak, A.M., and Kay, L.E. (2012). Proteasome allostery as a population shift between interchanging conformers. Proc. Natl. Acad. Sci. USA *109*, E3454–E3462.

Sijts, E.J.A.M., and Kloetzel, P.M. (2011). The role of the proteasome in the generation of MHC class I ligands and immune responses. Cell. Mol. Life Sci. *68*, 1491–1502.

Sijts, A.J.A.M., and Pamer, E.G. (1997). Enhanced intracellular dissociation of major histocompatibility complex class I-associated peptides: A mechanism for optimizing the spectrum of cell surface-presented cytotoxic T lymphocyte epitopes. J. Exp. Med. *185*, 1403–1411.

Sijts, A.J.A.M., Ruppert, T., Rehermann, B., Schmidt, M., Koszinowski, U., and Kloetzel, P.M. (2000). Efficient generation of a hepatitis B virus cytotoxic T lymphocyte epitope requires the structural features of immunoproteasomes. J. Exp. Med. *191*, 503–514.

Textoris-Taube, K., Keller, C., Liepe, J., Henklein, P., Sidney, J., Sette, A., Kloetzel, P.M., and Mishto, M. (2015). The T210M substitution in the HLA-A*02:01 gp100 epitope strongly affects overall proteasomal cleavage site usage and antigen processing. J. Biol. Chem. *290*, 30417–30428.

van der Burg, S.H., Visseren, M.J.W., Brandt, R.M.P., Kast, W.M., and Melief, C.J.M. (1996). Immunogenicity of peptides bound to MHC class I molecules depends on the MHC-peptide complex stability. J. Immunol. *156*, 3308–3314.

Vigneron, N., Stroobant, V., Chapiro, J., Ooms, A., Degiovanni, G., Morel, S., van der Bruggen, P., Boon, T., and Van den Eynde, B.J. (2004). An antigenic peptide produced by peptide splicing in the proteasome. Science *304*, 587–590.

Warren, E.H., Vigneron, N.J., Gavin, M.A., Coulie, P.G., Stroobant, V., Dalet, A., Tykodi, S.S., Xuereb, S.M., Mito, J.K., Riddell, S.R., and Van den Eynde, B.J. (2006). An antigen produced by splicing of noncontiguous peptides in the reverse order. Science *313*, 1444–1447.

Watson, A.M., Mylin, L.M., Thompson, M.M., and Schell, T.D. (2012). Modification of a tumor antigen determinant to improve peptide/MHC stability is associated with increased immunogenicity and cross-priming a larger fraction of CD8+ T cells. J. Immunol. *189*, 5549–5560.